Journal of Civil Engineering and Architecture 17 (2023) 484-492
doi: 10.17265/1934-7359/2023.10.002

Synthesis of Ceramic Tiles Reinforced with Addition of Aluminum Particulate Waste

Carla Tainara de Oliveira Lima, Rafael Pacheco Evangelista, Carlos Alberto França Junior, Aldemiro José Rocha Palma and Mirtânia Antunes Leão

Academic Department of Mechanical Technology, Federal Institute of Education, Science and Technology of Bahia, Campus Salvador, BA 40301-015, Brazil

Abstract: Research conducted on ceramic materials has been investigating the incorporation of solid waste into their formulations, driven by the proper disposal of such waste and the reduction of negative environmental impacts. This study analyzed the effects of adding aluminum powder residue to the physical properties of ceramic masses with the aim of obtaining new formulations for ceramic tiles. The aluminum residue and the standard mass for ceramic tile production were chemically characterized and homogenized to obtain new formulations with the incorporation of 4%, 6%, 8%, and 10% aluminum powder in the ceramic mass. The specimens were uniaxially pressed and sintered at a temperature of 1,200 °C for 2 h, undergoing three different temperatures (100 °C, 400 °C, and 650 °C) for 30 min each. They were evaluated for WA (water absorption), RLq (linear shrinkage), SEM (scanning electron microscopy), and TRF (flexural strength) modulus. The results demonstrate that the addition of aluminum powder residue is feasible in the proposed formulations (4%, 6%, 8%, and 10%), as they enhance the mechanical properties of the ceramics compared to the formulation with 0% residue, at a sintering temperature of 1,200 °C.

Key words: Ceramics, ceramic tiles, metallic waste, aluminum waste.

1. Introduction

The word "ceramic" comes from the Greek word "keramikos", which means "burnt material", indicating that the desirable properties of these materials are typically achieved through a sintering process. Their main characteristics include low thermal and electrical conductivity, high mechanical strength at elevated temperatures, and brittle behavior under stress [1].

Red ceramics derive their name from their primary component, clay, which commonly contains iron oxide—the element responsible for the characteristic reddish coloration in this type of ceramic. Clay-based materials encompass a range of porous ceramics, including bricks, tiles, earthenware, as well as glazed or vitrified ceramics like special bricks, tiles, and decorative tiles [2].

Pure aluminum, in contrast, is a lightweight metal with a white appearance, low hardness, high deformability, exceptional thermal and electrical conductivity, and a low melting point. Due to its strong reducing properties, aluminum undergoes oxidation when exposed to air, forming a thin layer of aluminum oxide that serves as a protective barrier against corrosion. Industrial aluminum products are supplied in various forms, including castings, sheets, tubes, profiles, and small-diameter wires. Within the construction industry, aluminum finds diverse applications such as window frames, doors, partitions, sheets for interior and exterior cladding, and roofing materials [3]. The manufacturing process of these products can generate waste, as is the case with aluminum shavings produced during the machining of aluminum profiles.

Mineral extraction and beneficiation create wealth for countries, but they also generate millions of tons of waste globally. The most common destinations for such

Corresponding author: Carla Tainara de Oliveira Lima, B. Mechanical Eng., research fields: composite materials, ceramics.

waste are industrial landfills, which tend to increase opportunity costs by not being reused, while also exacerbating environmental impact [4]. In this context, ceramic industries have been incorporating waste into their formulations, aiming to rationalize the use of natural resources and improve product properties. Shakir and Mohammed [5] reported on the state of the art in using various waste materials in brick manufacturing, such as foundry sand, granite sawdust, harbor sediments, perlite, sugarcane bagasse ash, chamotte, boron waste, sewage sludge, glass waste, among others. Due to the heterogeneity of ceramic products, a reasonable amount of waste can typically be incorporated without compromising their desired properties [6].

One of the types of ceramic products in which waste can be added is ceramic tile. The NBR ISO 13006/20 [7] standard defines ceramic tile "thin slab made from clays and/or other inorganic raw materials, generally used as covering for floors and walls, shaped (…) at room temperature, (…) then dried and subsequently fired at temperatures sufficient to develop the required properties".

This study aims to investigate the changes in the physical and mechanical properties of ceramic tiles due to the addition of different quantities of aluminum waste in powder form to their standard-mass.

2. Method and Materials

2.1 Raw Materials

2.1.1 Clay

For the development of this study, red clay provided by Cerâmica Candeias, located in the Metropolitan Region of Salvador, in the municipality of Candeias, Bahia, Brazil, was used. The clay's particle size distribution was suitable for achieving greater compactness when aluminum powder was added.

2.1.2 Aluminum Waste

The aluminum waste was obtained in the form of chips from profile manufacturing companies through machining processes (cutting, drilling, and bending). The waste was processed in a planetary ball mill and sieved to 270 mesh to achieve a better particle size distribution.

2.2 Raw Material Characterization

2.2.1 XRF (X-Ray Fluorescence) Chemical Analysis

XRF analysis was performed to identify the chemical elements present in the aluminum waste that had already been sieved to 270 mesh. The semi-quantitative XRF analysis was carried out using the BRUKER-S2 Ranger XRF equipment at the LCM (Materials Characterization Laboratory) of the IFBA (Federal Institute of Bahia), Salvador Campus.

2.3 Ceramic Production

2.3.1 Formulations

The standard mass and aluminum waste powder were manually homogenized following the mass quantities per specimen shown in Table 1. Subsequently, the mass was moistened and homogenized with the addition of 8% by mass of distilled water. Seven specimens were prepared for each formulation. The adopted standard mass consists of a mixture of red clay (40%), feldspar (40%), and kaolin (20%).

2.3.2 Specimen Preparation

The specimens were prepared using a manual press with a capacity of 15 t, located in the High-Energy Laboratory (Lab-MAE) at IFBA, Campus Salvador. The quenched SAE 1045 steel die measuring 60 ×20 × 5 mm was used, within this die, approximately 12 g (± 0.1 g) of ceramic material was placed. The compaction load applied was 5.0 t, and maintained for 1 min. Subsequently, the specimens were measured using a caliper with a resolution of 0.05 mm, weighed, and placed in a drying oven at 100 °C for 24 h. This drying process aimed to remove moisture and enhance the strength of the specimens before sintering.

Table 1 Formulations of ceramic masses.

Formulation (%)	Standard mass (g)	Aluminum mass (g)
0	12.00	0.00
4	11.52	0.48
6	11.28	0.72
8	11.04	0.96
10	10.80	1.20

2.3.3 Sintering

After drying, the specimens were sintered in a tubular electric furnace at a temperature of 1,200 °C for 2 h, with a heating rate of 5 °C/min. During the heating process, the specimens were held at each of the following temperature plateaus for 30 min: 100 °C, 400 °C, and 650 °C. The slow cooling was carried out within the closed furnace until reaching room temperature. After sintering, the specimens were measured and weighed once again for subsequent calculation of RLq (linear shrinkage upon firing) and water absorption (WA). Sintering was conducted in the furnace laboratory at IFBA, Campus Salvador.

2.4 Characterization of the Specimen after Sintering

The characterization of the specimens after sintering was determined experimentally through the following tests: RLq (linear shrinkage), WA (water absorption), TRF (flexural strength), and SEM (scanning electron microscopy).

2.4.1 RLq

After sintering, the specimens were measured to calculate the RLq using Eq. (1), where *Ls* is the length after drying (mm) and *Lq* is the length after sintering (mm):

$$RLq\ (\%) = \frac{Ls - Lq}{Lq}.100\% \quad (1)$$

2.4.2 WA

After sintering, the specimens were placed back in the drying oven at 100 °C for 24 h and weighed to obtain the dry mass (*Md*) for the calculation of WA. The values obtained for WA directly influence the material's strength. Subsequently, the specimens were immersed in distilled water for 24 h and weighed again to obtain the wet masses (*Mw*). Thus, the value of WA is calculated using Eq. (2):

$$WA\ (\%) = \frac{Mw - Md}{Md}.100\% \quad (2)$$

2.4.3 TRF

The three-point TRF test was conducted following ISO 10545-4/208 standard [8], with an application speed of 0.5 mm/min and a 50 mm distance between supports, The tests were performed on a universal testing machine, EMIC brand, model 23-20, located in the destructive testing laboratory at IFBA (Campus Salvador). To calculate the TRF, Eq. (3) is used, where "*F*" is the rupture load (N), "*L*" is the distance between the supports of the specimen (mm), "*b*" is the width of the specimen (mm), and "*e*" is the thickness of the specimen (mm).

$$TRF = \frac{3FL}{2be^2} \quad (3)$$

2.4.4 SEM

Microscopic analysis of the specimens was conducted after the TRF test to examine the fracture surface of the broken specimens. This analysis was performed using a scanning electron microscope, Tescan brand, model VEJA 3 LMU, at the Characterization Laboratory of IFBA (Campus Salvador).

3. Results and Discussions

3.1 Chemical Analysis by XRF

Table 2 presents the chemical composition of the aluminum residue sieved at 270 mesh, obtained through XRF analysis. It shows the presence of silicon dioxide (SiO_2) and aluminum oxide (Al_2O_3).

Table 2 Chemical composition of the materials.

Present elements	Concentration in weight %	
	Clay	Aluminum residue
SiO_2	56.27	-
Al_2O_3	27.89	76.92
K_2O	1.67	-
MgO	1.70	1.00
Na_2O	-	4.60
Fe_2O_3	10.41	0.13
P_2O_5	0.11	-
SO_3	0.20	-
TiO_2	1.39	10.09
ZrO_2	0.06	-
Cl	-	3.15

3.2 RLq (Linear Shrinkage)

Fig. 1 shows that the RLq is inversely proportional to the increase in aluminum content. The formulations from 0% to 6% had the highest shrinkage, while 8% and 10% had the lowest shrinkage. According to Biffi [9], the RLq in porcelain ceramics should be between 7% and 9%, and the values obtained in the 4% formulation fall within this range.

One hypothesis that explains the behavior of the specimens as more standard mass is replaced by aluminum residue is the loss of the characteristics of the compounds in the standard mass, such as the quartz in the clay and the formation of the liquid phase of the fluxes. In other words, despite aluminum having oxides that could perform this function, it did not behave as expected.

3.3 Water Absorption (WA)

Fig. 2 shows an increase in WA as the amount of aluminum residue increases. One of the reasons for this may be the low reactivity between metallic aluminum and the components of the ceramic mass during sintering at 1,200 °C, leading to the formation of voids between the metallic powder and the ceramic matrix.

Ceramics are classified according to their WA percentage and TRF, following NBR ISO 13006/20 [7] and the Sector Report No. 040/March/2022 from ANFACER [10]. This classification is reproduced in Table 3. The ceramic material exhibited increasing WA ranging from 1.97% to 10.51%. Along with the results of TRF, it is possible to determine the type of ceramics to which the produced formulations belong.

3.4 Flexural Strength (TRF)

Fig. 3 displays the values obtained from the TRF test.

As mentioned earlier, Table 3 displays the commercial classification of the ceramics based on the absorption and TRF groups according to the NBR ISO 13006/20 [7] standard. In this context, it was observed that the formulation with 0% aluminum, despite having a low

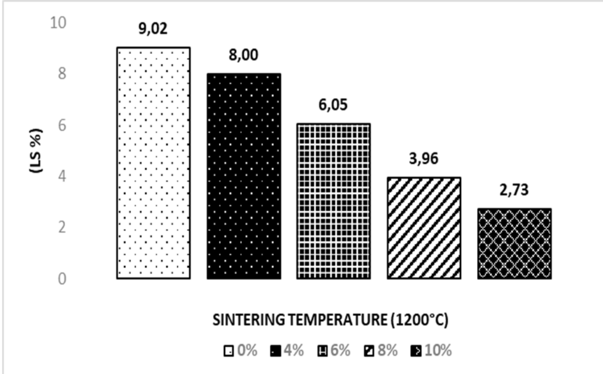

Fig. 1 RLq after sintering.

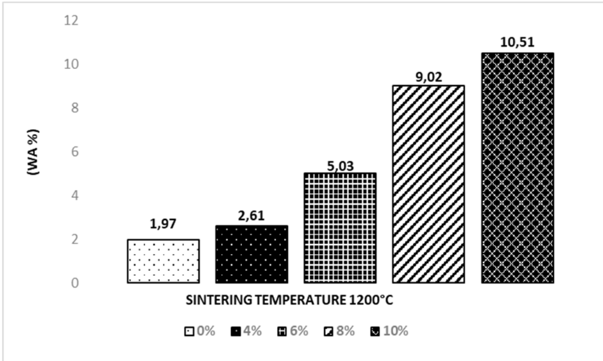

Fig. 2 WA after sintering.

Table 3 Commercial grade according to WA groups.

AA (%)	Technical Class	business class	Absorption	TRF (MPa)
Abs ≤ 0.5	AIa/BIa	Porcelain tile	Almost null	≥ 35
0.5 < Abs ≤ 3.0	AIb/BIb	Stoneware	Low	≥ 30
3.0 < Abs ≤ 6.0	AIIa/BIIA	Semi stoneware	Average	≥ 22
6.0 < Abs ≤ 10.0	AIIb/BIIb	Semi porous	Medium/ high	≥ 18
Abs > 10.0	AIII/BIII	Porous/monoporous	High	≥ 15

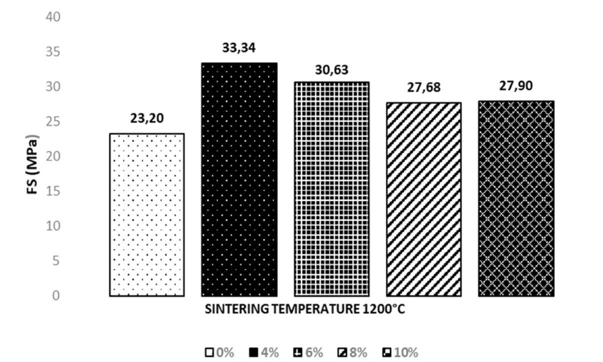

Fig. 3 Tensile bending stress after sintering.

Table 4 Commercial classification for each formulation.

Formulations (%)	Business class
-	Porcelain tile
4	Stoneware
6	Semi stoneware
8	Semi porous
10	Porous/monoporous

post-firing WA (1.97%), does not fall within the range required by the standard in terms of TRF (23.20 MPa). The other formulations, meeting the criteria for WA and TRF, comply with the standard and each falls into a different commercial class. The 4% formulation is classified as Stoneware (class BIb), the 6% formulation as Semi-stoneware (class BIIa), the 8% formulation as Semi-porous (class BIIb), and the 10% formulation as Porous/Monoporosa Class BIII. It is important to note that B represents the manufacturing method (pressed) and Ib/IIa/IIb/III represent the absorption group. It can be concluded that the formulations with 4%, 6%, 8%, and 10% exhibit significant values in terms of mechanical strength, meeting the requirements of the NBR ISO 13006/20 [7] standard. Table 4 provides a summary of the commercial classifications for each formulation based on their physical properties.

3.5 SEM

The microstructural characterization of the specimens was carried out through SEM analysis, after the sintering process at 1,200 °C, bending test and chemical attack with HF (hydrofluoric acid). It was possible to detect during the microstructural analysis the presence of glassy phases, pores, cracks, quartz, primary mullite crystals (volumetric format) and secondary mullite crystals (needle/acicular format). Fig. 4 shows the SEM image for the formulation with 0%, with magnifications of 1,000× and 5,000×, as well as its details.

It is possible to observe in Fig. 4 that in the region studied, pores, small cracks, gas bubbles, glassy phase, primary mullite, secondary mullite were found. It is possible to notice that in some cases the material was not completely sintered.

Figs. 5a and 5b show the SEM micrographs of the fractured surface, for the 4% formulation with approximations of 5,000× and 10,000×, as well as its details.

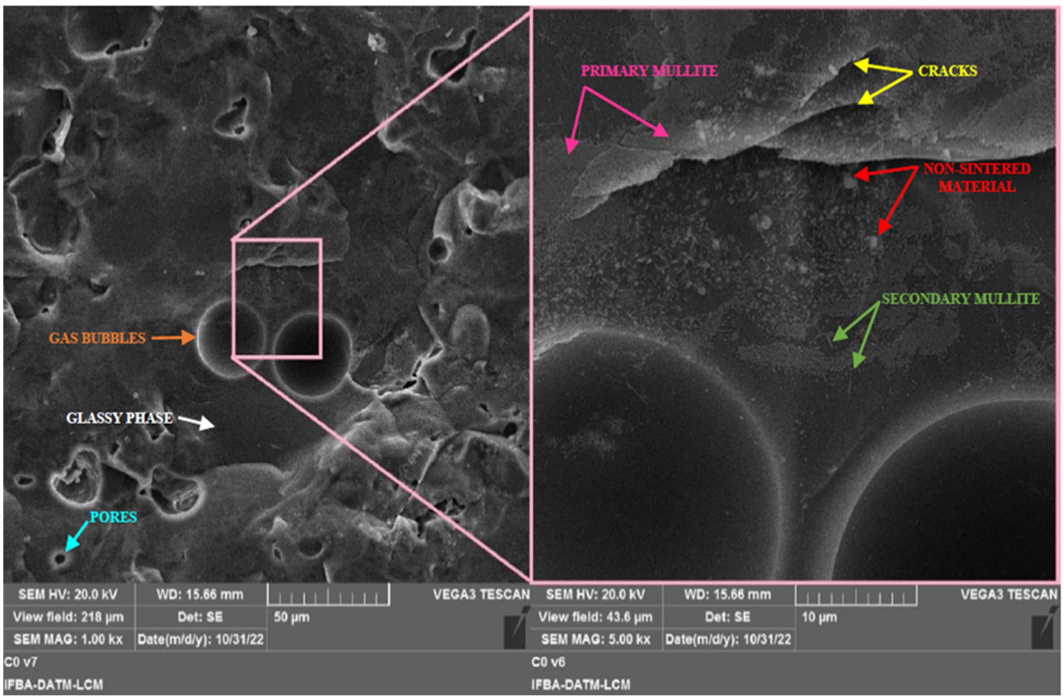

Fig. 4 Micrograph by SEM of the specimens with formulation 0%.

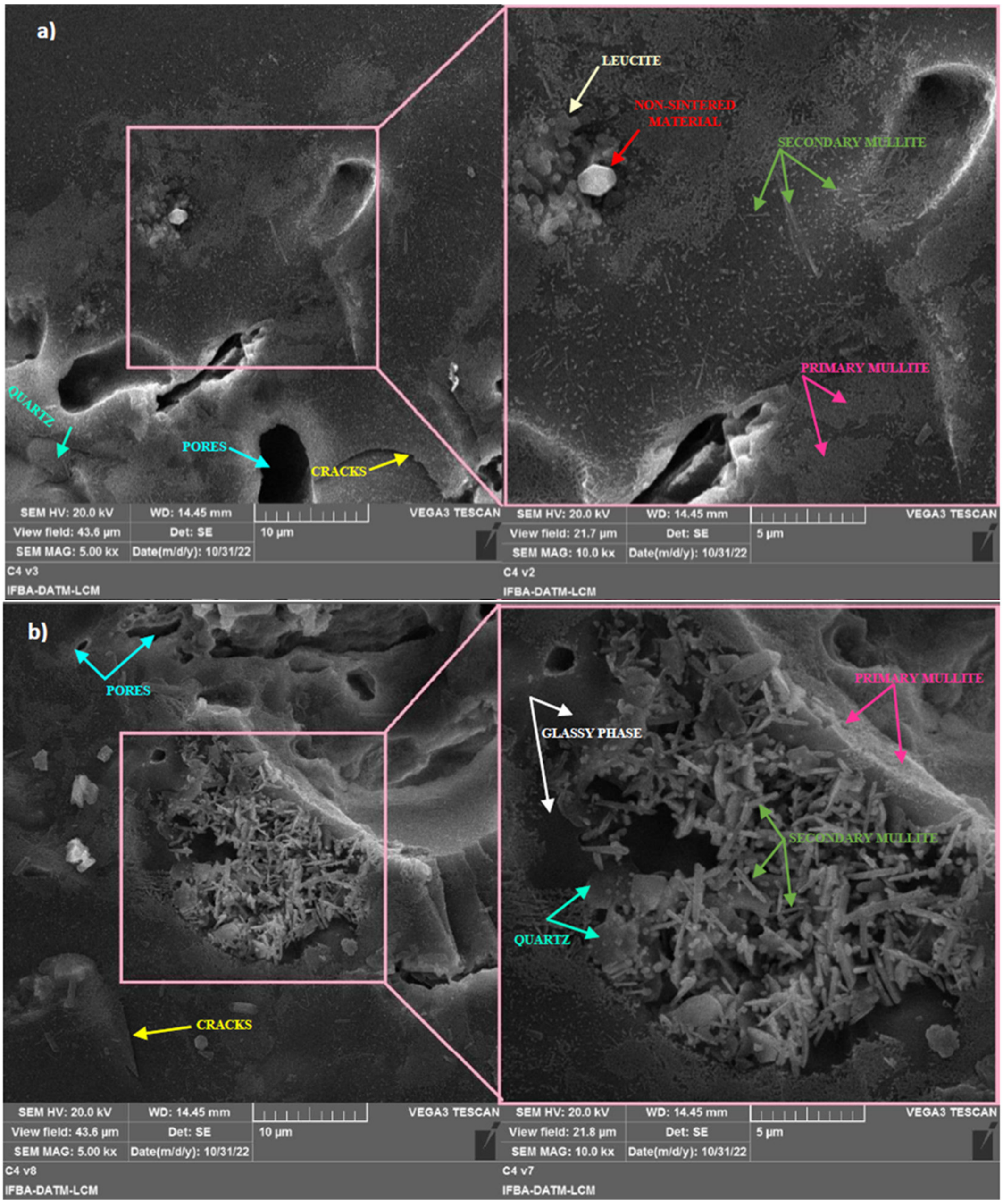

Fig. 5 Micrograph by SEM of the specimens with formulation 4%.

In the formulation with 4%, the presence of primary and secondary mullite in greater quantities can be noted. This formulation was the one that presented the highest TRF value. This can be directly linked to the smaller amount of pores found in the specimens, as well as their size, since the less pores are present inside the test specimen, the less the possibility of concentrating tension leading to the early rupture of the material, thus greater the mechanical resistance. In Fig. 5a, the appearance of more rounded quartz is observed. Quartz, when dissolved in feldspar, contributes to the formation of primary mullite. Therefore, there is formation of primary mullite in large amounts and also pores, cracks, non-sintered material and formation of secondary mullite. A crystal whose geometry resembles the leucite crystal was also found. In Fig. 5b, which shows another region of the same formulation, a large amount of acicular mullite of different interlaced sizes can be seen, which is another important factor for the increase in mechanical strength. Quartz appears around the primary and secondary mullite, and the presence of cracks and the vitreous phase are also observed.

Fig. 6 shows images obtained by SEM of the fracture surface of the 6% formulation, with magnifications of 5,000× and 10,000×. There is also the presence of cracks, vitreous phase and primary mullite in large quantities. Acicular mullite was also visualized, but in smaller quantities.

Fig. 7 shows images obtained by SEM of the fracture surface of the 8% formulation, with approximations of 5,000× and 10,000×. In the 8% formulation, a greater reduction of crystals is already observed, but even so, secondary and primary mullite is found, as well as pores, non-sintered material and a large crack, which may be related to the lower TRF obtained between the formulations.

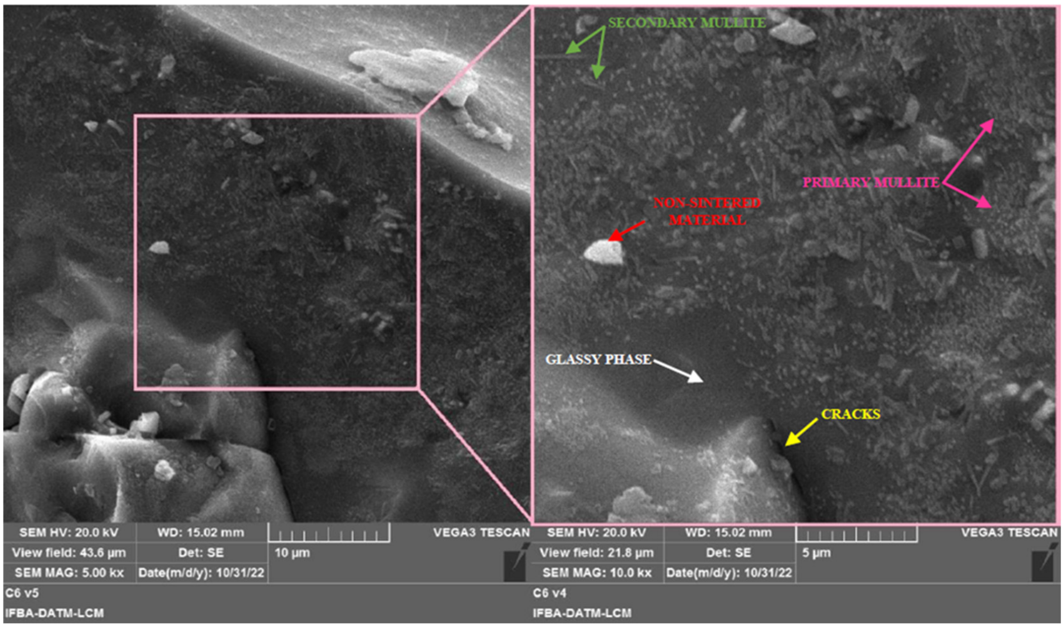

Fig. 6 Micrograph by SEM of the specimens with formulation 6%.

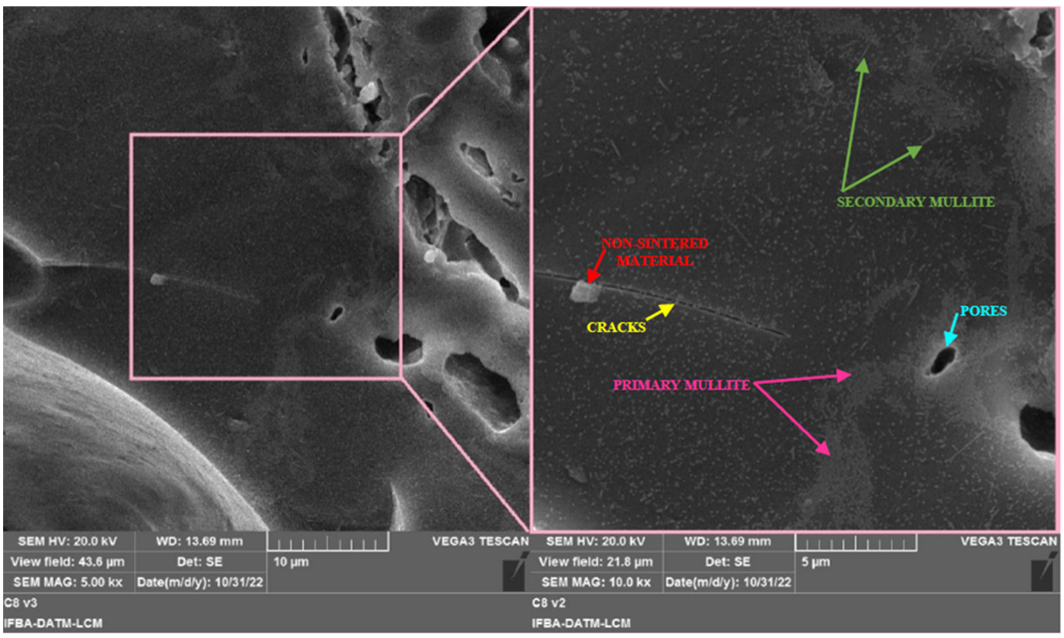

Fig. 7 Micrograph by SEM of the specimens with formulation 8%.

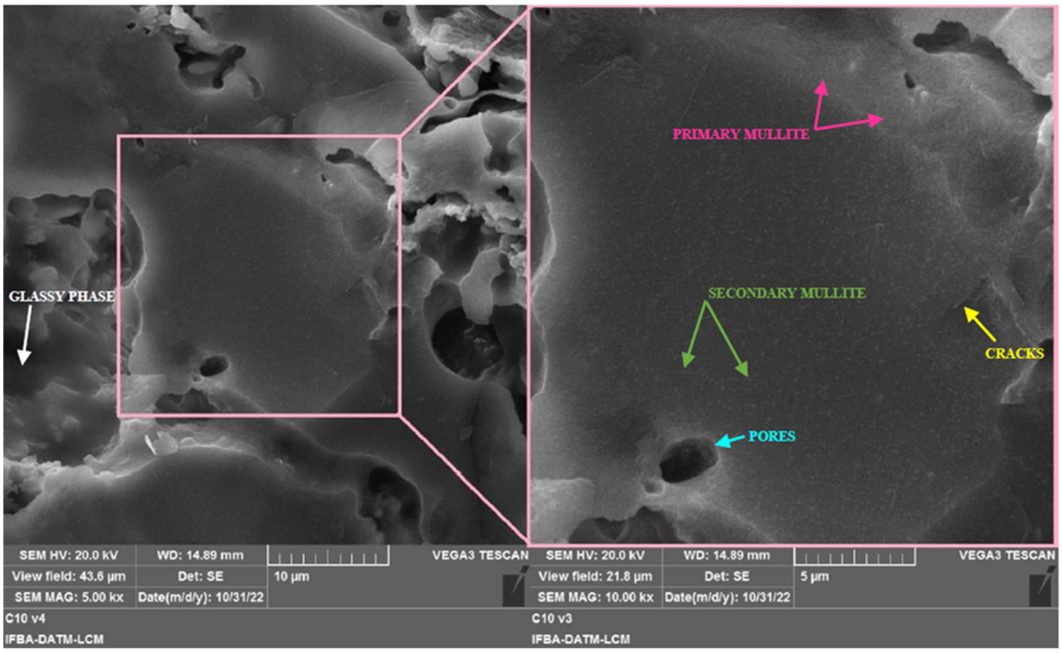

Fig. 8 Micrograph by SEM of the specimens with formulation 10%.

Fig. 8 shows images obtained by SEM of the fracture surface of the 10% formulation, with magnifications of 5,000× and 10,000×. Note that the concentration of flux, together with the amount of aluminum residue in the formulation, was not able to promote a large growth of secondary mullite during sintering, since most of the crystals were primary mullite. Vitreous phase, pores and cracks were also observed.

4. Conclusions

Based on the analysis of the results obtained for WA and TRF, it can be concluded that the addition of aluminum residue to the specimens was appropriate for the proposed formulations in relation to the values specified by the NBR ISO 13006/20 standard:

- All formulations with aluminum residue exhibited WA values ranging from 2.61% to 10.51%.
- The TRF modulus presented values between 27.68 MPa and 33.34 MPa.
- The 4% formulation showed the lowest WA (2.61% WA) and the highest TRF (33.34 MPa).

It was also observed that WA and RLq are inversely proportional. As aluminum residue is added to the formulation, RLq decreases while WA increases.

The studied material was classified as stoneware for the 4% formulation, semi-stoneware for 6%, semi-porous for 8%, and porous/monoporous for 10%. In this context, the addition of aluminum residue powder is viable for these formulations, as it improved the mechanical properties compared to the 0% formulation at a firing temperature of 1,200 °C, in accordance with NBR ISO 13006/20.

Acknowledgments

The authors would like to thank the Federal Institute of Education, Science and Technology of Bahia IFBA/PRPGI for financial support during this research project.

References

[1] Callister, J. R., and William, D. 2002. *Science and Engineering. Materials: An Introduction* (1st ed.). Rio de Janeiro: LTC. ISBN: 85-216-2188-5.

[2] Araújo, R. C. L. 2012. *Materiais de construção*. Juiz de Fora: McGrawHill. (in Portuguese)

[3] Smith, W. F., and Hashemi, J. 2012. *Fundamentos de Engenharia e Ciência dos Materiais* (5th ed.). Porto Alegre: McGrawHill. (in Portuguese)

[4] Brazilian Association of Waste Treatment Companies (ABETRE). 2003. *Overview of Industrial Waste Generation Estimates*. Final Report, São Paulo.

[5] Shakir, A. A., and Mohammed, A. A. 2013. "Manufacturing of Bricks in the Past, in the Present and in the Future: A State of the Art Review." *International Journal of Advances in Applied Sciences* 2 (3): 145-56.

[6] Segadães, A. M. 1987. Equilibrium *Phase Diagrams: Theory and Applications in Ceramics.* São Paulo: Edgard Blücher Ltda.

[7] Brazilian Association of Technical Standards. 2020. *NBR ISO 13006/12 2020: Ceramic Tiles—Definitions, Classification, Characteristics and Marking*. Rio de Janeiro: ABNT.

[8] Standard ISO 10545-4/07 2020. *Breaking Strength*.

[9] Biffi, G. 2002. *Porcelain Stoneware: Manufacturing Manual and Employment Techniques*, edited by Faenza. S. Paulo: Editrice do Brasil.

[10] ANFACER (National Association of Ceramic Coating Manufacturers). 2022. *Sectorial Report No. 040/March/2022*.